Anal. Chem. **2002,** *74,* 3168−3173

Genotyping on a Complementary Metal Oxide Semiconductor Silicon Polymerase Chain Reaction Chip with Integrated DNA Microarray

Dieter Trau,[†,‡] Thomas M. H. Lee,[§] Alex I. K. Lao,[§] Ralf Lenigk,[†] I-Ming Hsing,[§] Nancy Y. Ip,[†,‡] Maria C. Carles,[†,‡] and Nikolaus J. Sucher*[,†,⊥]

Biotechnology Research Institute and Departments of Biochemistry, Chemical Engineering, and Biology, Hong Kong University of Science and Technology, Hong Kong SAR, China

A novel method for the fast identification of genetic material utilizing a micro-DNA amplification and analysis device (*μ*-DAAD) consisting of multiple PCR microreactors with integrated DNA microarrays was developed. The device was fabricated in Si-technology and used for the genotyping of Chinese medicinal plants on the basis of differences in the noncoding region of the 5S-rRNA gene. Successful amplification of the genetic material and the consecutive analysis of the fluorescent-labeled amplicons in the *μ*-DAAD by the integrated oligonucleotide probes were demonstrated. Parallel analysis was performed by loading the four PCR reactors of the *μ*-DAAD with different samples of 3-*μ*L volume. Temperature sensors and heating elements of the *μ*-DAAD enable precise temperature control and fast cycling, allowing the rapid completion of a combined amplification and analysis (hybridization) experiment.

The flood of data resulting from genome sequencing projects such as the human genome project[1,2] fostered the development of DNA microarrays.[3] Today, two types of DNA microarrays find widespread application: microarrays for (genome-wide) expression profiling and microarrays for genotyping and single nucleotide polymorphism (SNP) detection.[4] Their use in research, clinical environments, forensics, point-of-care, and pharmacogenetics holds great promise. For genotyping and SNP detection, PCR amplification is usually needed in the sample preparation procedure before the sample is analyzed by hybridization to oligonucleotide probes of the array. Methods that are currently in use have the drawback that they are relatively slow and require manual liquid transfer and, therefore, larger reagent and sample volumes. Moreover, sample transport of small volumes is difficult. Therefore, the integration of PCR with an analytical method for its analysis in a single device would be of great value, both scientifically and commercially. Obtaining information about the amount of PCR product, its length, and its sequence during or after the PCR reaction is of interest. Real-time fluorescence measurement of DNA production was reported by Nortrup et al.[5] The method has the advantage of monitoring the PCR, but no information about amplicon length and sequence is obtained. Wooley et al.[6] reported the integration of microelectrophoresis onto a silicon-based PCR chip. This method provides analysis of amplicon length in real-time or after the PCR reaction. Multiple PCR products can be identified by their length difference, but no sequence data is obtained.

* Corresponding author. E-mail: sucher@ust.hk.
† Biotechnology Research Institute.
‡ Department of Biochemistry.
§ Department of Chemical Engineering.
⊥ Department of Biology.

(1) Venter, J. C.; Adams, M. D.; Myers, E. W.; Li, P. W.; Mural, R. J.; Sutton, G. G.; Smith, H. O.; Yandell, M.; Evans, C. A.; Holt, R. A.; Gocayne, J. D.; Amanatides, P.; Ballew, R. M.; Huson, D. H.; Wortman, J. R.; Zhang, Q.; Kodira, C. D.; Zheng, X. H.; Chen, L.; Skupski, M.; Subramanian, G.; Thomas, P. D.; Zhang, J.; Gabor Miklos, G. L.; Nelson, C.; Broder, S.; Clark, A. G.; Nadeau, J.; McKusick, V. A.; Zinder, N.; Levine, A. J.; Roberts, R. J.; Simon, M.; Slayman, C.; Hunkapiller, M.; Bolanos, R.; Delcher, A.; Dew, I.; Fasulo, D.; Flanigan, M.; Florea, L.; Halpern, A.; Hannenhalli, S.; Kravitz, S.; Levy, S.; Mobarry, C.; Reinert, K.; Remington, K.; Abu-Threideh, J.; Beasley, E.; Biddick, K.; Bonazzi, V.; Brandon, R.; Cargill, M.; Chandramouliswaran, I.; Charlab, R.; Chaturvedi, K.; Deng, Z.; Di Francesco, V.; Dunn, P.; Eilbeck, K.; Evangelista, C.; Gabrielian, A. E.; Gan, W.; Ge, W.; Gong, F.; Gu, Z.; Guan, P.; Heiman, T. J.; Higgins, M. E.; Ji, R. R.; Ke, Z.; Ketchum, K. A.; Lai, Z.; Lei, Y.; Li, Z.; Li, J.; Liang, Y.; Lin, X.; Lu, F.; Merkulov, G. V.; Milshina, N.; Moore, H. M.; Naik, A. K.; Narayan, V. A.; Neelam, B.; Nusskern, D.; Rusch, D. B.; Salzberg, S.; Shao, W.; Shue, B.; Sun, J.; Wang, Z.; Wang, A.; Wang, X.; Wang, J.; Wei, M.; Wides, R.; Xiao, C.; Yan, C.; Yao, A.; Ye, J.; Zhan, M.; Zhang, W.; Zhang, H.; Zhao, Q.; Zheng, L.; Zhong, F.; Zhong, W.; Zhu, S.; Zhao, S.; Gilbert, D.; Baumhueter, S.; Spier, G.; Carter, C.; Cravchik, A.; Woodage, T.; Ali, F.; An, H.; Awe, A.; Baldwin, D.; Baden, H.; Barnstead, M.; Barrow, I.; Beeson, K.; Busam, D.; Carver, A.; Center, A.; Cheng, M. L.; Curry, L.; Danaher, S.; Davenport, L.; Desilets, R.; Dietz, S.; Dodson, K.; Doup, L.; Ferriera, S.; Garg, N.; Gluecksmann, A.; Hart, B.; Haynes, J.; Haynes, C.; Heiner, C.; Hladun, S.; Hostin, D.; Houck, J.; Howland, T.; Ibegwam, C.; Johnson, J.; Kalush, F.; Kline, L.; Koduru, S.; Love, A.; Mann, F.; May, D.; McCawley, S.; McIntosh, T.; McMullen, I.; Moy, M.; Moy, L.; Murphy, B.; Nelson, K.; Pfannkoch, C.; Pratts, E.; Puri, V.; Qureshi, H.; Reardon, M.; Rodriguez, R.; Rogers, Y. H.; Romblad, D.; Ruhfel, B.; Scott, R.; Sitter, C.; Smallwood, M.; Stewart, E.; Strong, R.; Suh, E.; Thomas, R.; Tint, N. N.; Tse, S.; Vech, C.; Wang, G.; Wetter, J.; Williams, S.; Williams, M.; Windsor, S.; Winn-Deen, E.; Wolfe, K.; Zaveri, J.; Zaveri, K.; Abril, J. F.; Guigo, R.; Campbell, M. J.; Sjolander, K. V.; Karlak, B.; Kejariwal, A.; Mi, H.; Lazareva, B.; Hatton, T.; Narechania, A.; Diemer, K.; Muruganujan, A.; Guo, N.; Sato, S.; Bafna, V.; Istrail, S.; Lippert, R.; Schwartz, R.; Walenz, B.; Yooseph, S.; Allen, D.; Basu, A.; Baxendale, J.; Blick, L.; Caminha, M.; Carnes-Stine, J.; Caulk, P.; Chiang, Y. H.; Coyne, M.; Dahlke, C.; Mays, A.; Dombroski, M.; Donnelly, M.; Ely, D.; Esparham, S.; Fosler, C.; Gire, H.; Glanowski, S.; Glasser, K.; Glodek, A.; Gorokhov, M.; Graham, K.; Gropman, B.; Harris, M.; Heil, J.; Henderson, S.; Hoover, J.; Jennings, D.; Jordan, C.; Jordan, J.; Kasha, J.; Kagan, L.; Kraft, C.; Levitsky, A.; Lewis, M.; Liu, X.; Lopez, J.; Ma, D.; Majoros, W.; McDaniel, J.; Murphy, S.; Newman, M.; Nguyen, T.; Nguyen, N.; Nodell, M.; Pan, S.; Peck, J.; Peterson, M.; Rowe, W.; Sanders, R.; Scott, J.; Simpson, M.; Smith, T.; Sprague, A.; Stockwell, T.; Turner, R.; Venter, E.; Wang, M.; Wen, M.; Wu, D.; Wu, M.; Xia, A.; Zandieh, A.; Zhu, X. *Science* **2001**, *291*, 1304−1351.

10.1021/ac020053u CCC: $22.00
Published on Web 05/23/2002

The integration of a microarray into a PCR reactor has the advantage of obtaining sequence data for PCR product analysis and identification. Furthermore, a high number of different PCR products can be distinguished in parallel, thus providing genotyping capabilities.

This approach is demonstrated here in a micro-DNA amplification and analysis device (μ-DAAD). This device consists of multiple PCR microreactors with integrated oligonucleotide microarrays. Both the amplification of target DNA sequences in a PCR microreactor and their consecutive analysis in a hybridization assay are performed inside the reactor chamber. The hybridization assay was performed on an integrated oligonucleotide microarray printed onto the bottom wall of the PCR microreactor chamber. This novel method combines PCR with a hybridization assay on a single chip. No buffer exchange or sample transfer is needed, thus reducing assay time and contamination risk. Using this device, we have developed an assay that allows the rapid identification of genetic material. A region of interest of a gene is amplified by an asymmetric PCR reaction, and the PCR products are analyzed by a microarray inside the PCR chamber.

EXPERIMENTAL SECTION

PCR Microreactor Production. The device was fabricated in a CMOS-compatible process on 100-mm, *n*-type Si (100) wafers. Microreactors with integrated heaters and temperature sensors for real-time temperature monitoring and control were produced by a process similar to that described previously.[7] A single device contained 4 PCR microreactors of 3 μL internal volume. A microarray was printed onto the bottom of each microreactor, and the chambers were closed by bonding a glass wafer with holes for reagent injection onto the silicon wafer (described later in this section).

Surface Treatment and Microarray Printing. The wafer was treated with a solution of ammonium hydroxide (25%), hydrogen peroxide (30%), and water (1:1:5) for 24 h at room temperature to hydroxylate the silicon dioxide surface in the reactor cavities. After washing with ddH_2O and drying, the surface was silanized with pure mercaptopropyl trimethoxysilane (MPTS) at 80 °C in a nitrogen atmosphere for 30 min. The wafer was rinsed with abs 2-propanol then with ddH_2O and dried with nitrogen gas. The 5′ SH−terminated oligonucleotides (Synthetic Genetics, CA) used as probes or immobilization controls were spotted into the cavity of the MPTS-coated microreactor. Oligonucleotides were diluted to a concentration of 20 μM in spotting buffer (2× saline−sodium citrate buffer (SSC) pH 7.3, 10% dimethyl sulfoxide (DMSO)). The SSC buffer was made from a stock solution of 20× SSC containing 3 M NaCl and 0.3 M sodium citrate adjusted to pH 7.3 with 1 M HCl. Six columns, each containing 4 spots of the oligonucleotides nos. 23, 28, 33, 42, 88, and 10 (from left to right) and one column of spotting buffer before and after the oligonucleotide columns, were spotted using a microcontact printer (Cartesian Technologies, Irvine, CA). The microcontact tip (Arraylt SMP3, 100-μm diameter, TeleChem International Inc., CA) was washed after each sample in 2× SSC containing 1% sodium dodecyl sulfate (SDS) and then in ddH_2O using an automated washing station. To prevent drying of the solutions, the printing was carried out at 80% relative humidity. The printed wafer was incubated overnight (∼12 h) in a closed wafer box containing 50 μL of water to create a humidified atmosphere. Nonimmobilized oligonucleotides were washed off with 10 mM Tris pH 7.5, 0.5% Tween-20 for 40 min at 60 °C and then with ddH_2O. Finally, the wafer was dried using nitrogen gas.

Bonding. A cover glass wafer (Corning 7740, Corning, NY) with inlet and outlet holes at the corresponding diagonal corner positions of each microreactor cavity was bonded to the silicon wafer. The glass wafer was silanized prior bonding by treatment with pure trimethoxymethylsilane in a nitrogen gas atmosphere for 30 min at 80 °C, then washed with abs 2-propanol and dried under nitrogen gas. A small amount of UV glue (Sk-9, Summers Optical, PA) was distributed onto the entire surface (except the cavities) of the silicon wafer. The holes of the glass wafer were aligned with the reactor cavities, and slight pressure was applied. A mask (chromium on glass) was placed onto the wafer sandwich to protect the immobilized oligonucleotides from UV light. The

(2) Lander, E. S.; Linton, L. M.; Birren, B.; Nusbaum, C.; Zody, M. C.; Baldwin, J.; Devon, K.; Dewar, K.; Doyle, M.; FitzHugh, W.; Funke, R.; Gage, D.; Harris, K.; Heaford, A.; Howland, J.; Kann, L.; Lehoczky, J.; LeVine, R.; McEwan, P.; McKernan, K.; Meldrim, J.; Mesirov, J. P.; Miranda, C.; Morris, W.; Naylor, J.; Raymond, C.; Rosetti, M.; Santos, R.; Sheridan, A.; Sougnez, C.; Stange-Thomann, N.; Stojanovic, N.; Subramanian, A.; Wyman, D.; Rogers, J.; Sulston, J.; Ainscough, R.; Beck, S.; Bentley, D.; Burton, J.; Clee, C.; Carter, N.; Coulson, A.; Deadman, R.; Deloukas, P.; Dunham, A.; Dunham, I.; Durbin, R.; French, L.; Grafham, D.; Gregory, S.; Hubbard, T.; Humphray, S.; Hunt, A.; Jones, M.; Lloyd, C.; McMurray, A.; Matthews, L.; Mercer, S.; Milne, S.; Mullikin, J. C.; Mungall, A.; Plumb, R.; Ross, M.; Shownkeen, R.; Sims, S.; Waterston, R. H.; Wilson, R. K.; Hillier, L. W.; McPherson, J. D.; Marra, M. A.; Mardis, E. R.; Fulton, L. A.; Chinwalla, A. T.; Pepin, K. H.; Gish, W. R.; Chissoe, S. L.; Wendl, M. C.; Delehaunty, K. D.; Miner, T. L.; Delehaunty, A.; Kramer, J. B.; Cook, L. L.; Fulton, R. S.; Johnson, D. L.; Minx, P. J.; Clifton, S. W.; Hawkins, T.; Branscomb, E.; Predki, P.; Richardson, P.; Wenning, S.; Slezak, T.; Doggett, N.; Cheng, J. F.; Olsen, A.; Lucas, S.; Elkin, C.; Uberbacher, E.; Frazier, M.; Gibbs, R. A.; Muzny, D. M.; Scherer, S. E.; Bouck, J. B.; Sodergren, E. J.; Worley, K. C.; Rives, C. M.; Gorrell, J. H.; Metzker, M. L.; Naylor, S. L.; Kucherlapati, R. S.; Nelson, D. L.; Weinstock, G. M.; Sakaki, Y.; Fujiyama, A.; Hattori, M.; Yada, T.; Toyoda, A.; Itoh, T.; Kawagoe, C.; Watanabe, H.; Totoki, Y.; Taylor, T.; Weissenbach, J.; Heilig, R.; Saurin, W.; Artiguenave, F.; Brottier, P.; Bruls, T.; Pelletier, E.; Robert, C.; Wincker, P.; Smith, D. R.; Doucette-Stamm, L.; Rubenfield, M.; Weinstock, K.; Lee, H. M.; Dubois, J.; Rosenthal, A.; Platzer, M.; Nyakatura, G.; Taudien, S.; Rump, A.; Yang, H.; Yu, J.; Wang, J.; Huang, G.; Gu, J.; Hood, L.; Rowen, L.; Madan, A.; Qin, S.; Davis, R. W.; Federspiel, N. A.; Abola, A. P.; Proctor, M. J.; Myers, R. M.; Schmutz, J.; Dickson, M.; Grimwood, J.; Cox, D. R.; Olson, M. V.; Kaul, R.; Shimizu, N.; Kawasaki, K.; Minoshima, S.; Evans, G. A.; Athanasiou, M.; Schultz, R.; Roe, B. A.; Chen, F.; Pan, H.; Ramser, J.; Lehrach, H.; Reinhardt, R.; McCombie, W. R.; de la Bastide, M.; Dedhia, N.; Blocker, H.; Hornischer, K.; Nordsiek, G.; Agarwala, R.; Aravind, L.; Bailey, J. A.; Bateman, A.; Batzoglou, S.; Birney, E.; Bork, P.; Brown, D. G.; Burge, C. B.; Cerutti, L.; Chen, H. C.; Church, D.; Clamp, M.; Copley, R. R.; Doerks, T.; Eddy, S. R.; Eichler, E. E.; Furey, T. S.; Galagan, J.; Gilbert, J. G.; Harmon, C.; Hayashizaki, Y.; Haussler, D.; Hermjakob, H.; Hokamp, K.; Jang, W.; Johnson, L. S.; Jones, T. A.; Kasif, S.; Kaspryzk, A.; Kennedy, S.; Kent, W. J.; Kitts, P.; Koonin, E. V.; Korf, I.; Kulp, D.; Lancet, D.; Lowe, T. M.; McLysaght, A.; Mikkelsen, T.; Moran, J. V.; Mulder, N.; Pollara, V. J.; Ponting, C. P.; Schuler, G.; Schultz, J.; Slater, G.; Smit, A. F.; Stupka, E.; Szustakowski, J.; Thierry-Mieg, D.; Thierry-Mieg, J.; Wagner, L.; Wallis, J.; Wheeler, R.; Williams, A.; Wolf, Y. I.; Wolfe, K. H.; Yang, S. P.; Yeh, R. F.; Collins, F.; Guyer, M. S.; Peterson, J.; Felsenfeld, A.; Wetterstrand, K. A.; Patrinos, A.; Morgan, M. J.; Szustakowki, J. *Nature* **2001**, *409*, 860−921.

(3) Schena, M. *DNA Microarrays: a Practical Approach*; Oxford University Press: Oxford; Hong Kong, 1999.

(4) Thompson, M.; Furtado, L. M. *Analyst* **1999**, *124*, 1133−1136.

(5) Northrup, M. A.; Benett, B.; Hadley, D.; Landre, P.; Lehew, S.; Richards, J.; Stratton, P. *Anal. Chem*. **1998**, *70*, 918−922.

(6) Woolley, A. T.; Hadley, D.; Landre, P.; deMello, A. J.; Mathies, R. A.; Northrup, M. A. *Anal. Chem*. **1996**, *68*, 4081−4086.

(7) Lee, T. M.; Hsing, I. M.; Lao, A. I.; Carles, M. C. *Anal. Chem*. **2000**, *72*, 4242−4247.

wafer was exposed for 3 h to UV light (254 nm, Spectroline, NY). In addition the wafer was treated at 80 °C in the vacuum (20 mbar) for 2 h in order to remove or inactivate uncured UV-glue components such as solvents or other low molecular weight components resulting from incomplete curing, which were found to inhibit the PCR. The inlet and outlet holes were sealed with adhesive tape (3M 5419, 3M Corporation, MN) and the wafer was diced into 16 μ-DAAD's with a diamond saw.

PCR Mix Preparation. The PCR mixture contained 1.25 U Taq DNA polymerase/50 μL, 0.08−0.4 μM of each fluorescently labeled reverse primer (nos. 26, 85), 4 nM of each forward primer (nos. 25, 91), 2 mM magnesium chloride, 0.2 mM of each dNTP, 1× Taq buffer, and 0.5 μg/μL BSA (primers were purchased from Synthetic Genetics; CA and PCR reagents, from Promega, WI). An amount of 15 pg−50 ng of DNA template (pGEM-T Easy 5S-rRNA spacer domain from *Pinellia padatisecta* or *Datura innoxia*)/50 μL of master mix (1 ng pGEM-T Easy vector is equivalent to ~0.5 fmol) was added. A volume of ~3 μL PCR mix was loaded bubble-free into each PCR reactor (0.3 pg−3 ng template per reactor). The cover glass holes were sealed with adhesive tape (3M 5419, 3M Corporation, MN). A second tape was used to provide heat insulation to the probe station.

System Setup and Parameters. The on-chip resistance temperature sensors and heaters were connected via a probe station (PM 5, Carl Suss, Germany). A PC running LabVIEW 6i (National Instruments, TX) software was used for temperature measurement and control. The signal of the temperature sensors was acquired using a data acquisition card (PCI-MIO-16E-1, National Instruments, TX) and a signal conditioning board (SC-2042-RTD, National Instruments, TX) and converted to temperature values by using a calibration curve. The heaters were connected to a PC-controlled external power supply (HP6629A, Hewlett-Packard, CA) to heat the device to the desired PCR cycle set-point temperature. The PCR cycle set-point temperatures were set as follows: initial denaturation, 94 °C for 300 s (denaturation, 94 °C for 60 s; annealing, 50 °C for 60 s; elongation, 70 °C for 60 s) × 30−36 cycles. Following PCR, the samples were hybridized at 48−50 °C for at least 3 h.

Fluorescence Detection and Assay Readout. After completion of the combined PCR and hybridization experiment, the device was disconnected from the probe station, and the reactor chambers were washed with 2× SSC containing 0.1% SDS for 2 min at 48 °C and then with ddH_2O for 30 s at room temperature. A vacuum was used to fill in and remove the washing solution. The reaction chambers were dried with nitrogen gas, and the device was mounted onto a microscope slide. The focal plane of the laser scanner (ScanArray 5000, Packard Biosciences, CT) was adjusted to the reaction chamber bottom. The arrays were scanned through the cover glass plate with Texas Red laser and filter settings (excitation wavelength, 594 nm; emission wavelength, 614 nm) at a resolution of 5 μm. The spot intensity was measured with QuantArray (Packard biosciences, CT) evaluation software. In general, background signals originated from (i) unspecific binding of any component onto the surface (spot and nonspot area) and (ii) binding of the PCR product onto oligonucleotide spots that was caused by unspecific hybridization or interaction. The former source of background signals was reduced as much as possible by blocking agents; the latter, by stringent hybridization/washing conditions. We defined the noise as unspecific hybridization/binding of the PCR products to spots corresponding to a nontarget species.

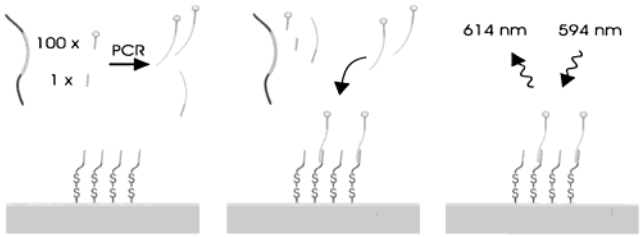

Figure 1. Schematic illustration of the assay principle performed in the μ-DAAD: (A) Asymmetric PCR reaction. A ratio of 100:1 was chosen between the fluorescent-labeled primer (designated as 100×) and the nonlabeled primer (designated as 1×) to generate an excess of the fluorescent-labeled PRC product. (B) Hybridization of the fluorescent-labeled amplicons onto the DNA array probes. (C) Separation of nonhybridized DNA and fluorescence detection (excitation wavelength, 594 nm; emission wavelength, 614 nm).

RESULTS AND DISCUSSION

The assay principle is depicted in Figure 1. The target DNA derived from traditional Chinese medicinal plants (TCMs) was amplified, and one amplicon strand was labeled by using a fluorescence-labeled reverse primer (Figure 1A). To ensure that the fluorescent-labeled strand hybridized with the array and not with its complementary amplicon, an asymmetric PCR was carried out. A ratio of 100:1 between the fluorescent-labeled reverse primer and the forward primer was chosen to produce an excess of the fluorescent-labeled amplicon strand. Subsequently, the labeled strand was hybridized to the integrated oligonucleotide array (Figure 1B). After nonhybridized DNA was washed away, the presence of the target DNA was detected by fluorescence scanning (Figure 1C). The assay principle described above was demonstrated for the genotyping of Chinese medicinal herbs. The gene coding for the 5S-rRNA was used as the template in the PCR amplification and was used for identification purposes as previously described.[8,9] Species-specific sequences of the 5S-rRNA gene were used to design primers (Table 1) for the selective amplification of 60- to 200-bp target fragments.

Device Fabrication. All μ-DAAD production steps were carried out wafer-based. Figure 2A shows a 100-mm *n*-type Si (100) wafer with 16 devices, each carrying 4 microreactors. Reactors ($2.5 \times 3.5 \times 0.35$ mm^3) were etched using concentrated potassium hydroxide solution, leaving only a membrane of 150 μm silicon to the rear side with the platinum heater and temperature sensor structures (Figure 2C). The 150-μm silicon membrane is mechanically stable and provides a quick heat transfer to the PCR reaction mixture. A top layer of 500 Å of silicon dioxide was grown on the front side of the wafer to enable the covalent attachment of mercaptopropyl trimethoxysilane, used as a bifunctional linker for the immobilization of oligonucleotides.[10] The oligonucleotide microarrays were printed into the PCR microreactor chambers of the wafer. Thiol-modified oligonucleotides were contact-printed

(8) Cai, Z. H.; Li, P.; Dong, T. T.; Tsim, K. W. *Planta Med.* **1999**, *65*, 360−364.
(9) Carles, M.; Lee, T.; Moganti, S.; Lenigk, R.; Tsim, K. W.; Ip, N. Y.; Hsing, I. M.; Sucher, N. J. *Fresenius' J. Anal. Chem.* **2001**, *371*, 190−194.
(10) Lenigk, R.; Carles, M.; Ip, N. Y.; Sucher, N. J. *Langmuir* **2001**, *17*, 2497−2501.

Table 1. Oligonucleotide Sequences, Purpose, and Modifications

oligonucleotide	purpose	modification	length	% GC
Pinellia padatisecta (PP)				
no. 23 TTGCCGCATGTCCCATTTTT	immobilization	SH−C18 at 5′	20	45
no. 25 TTGCCGCATGTCCCATTTTT	fwd-primer	none	20	45
no. 26 CCGAGTCTGCTTTCC	rvs primer	Texas Red at 5′	15	60
Datura innoxia (DI)				
no. 88 AGCTAGCTGGGTCTTCGTGTTGCATCCCGCT	immobilization	SH-C18 at 5′	31	58
no. 91 AGCTAGCTGGGTCTTCGTGTTGCATCCCGCT	fwd primer	none	31	58
no. 85 TAACGACACCCCGCCCCGAA	rvs primer	Texas Red at 5′	20	65
Alocasia macrorrhiza (AM)				
no. 28 TGCGCAATTTTTTTGAAAAG	immobilization	SH-C18 at 5′	20	30
Typhonium giganteum (TG)				
no. 33 ATCCCATCACCTGCATGGAC	immobilization	SH-C18 at 5′	20	55
Hemerocallis fulva (HF)				
no. 42 ATCCGGAATTATGTTTTGCCGGA	immobilization	SH-C18 at 5′	23	43
immobilization control				
no. 10 GTGCTTGGGCGA	immobilization	SH-C18 at 5′; Texas Red at 3′	12	67

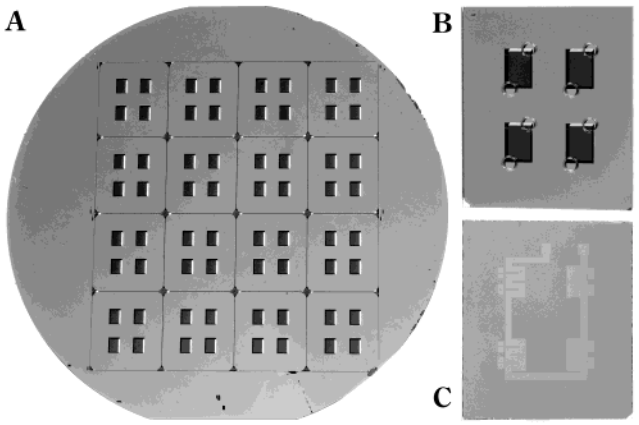

Figure 2. Photographs of μ-DAAD production steps: (A) Front side of a 4-in. silicon wafer with etched microreactors; 16 μ-DAAD are processed in parallel, each consisting of four microreactors. (B) Front side of a single μ-DAAD (16 × 18 mm^2) after bonding of a cover glass wafer and dicing. DNA arrays are printed onto the bottom of the microreactor cavities, but cannot be seen in this image because of their small size. Holes of 1 mm in diameter are drilled in the cover glass for the filling of the μ-DAAD reactors with reagent. (C) Backside of the device with platinum heater coil and thermoresistors placed at the corresponding area of the microreactor.

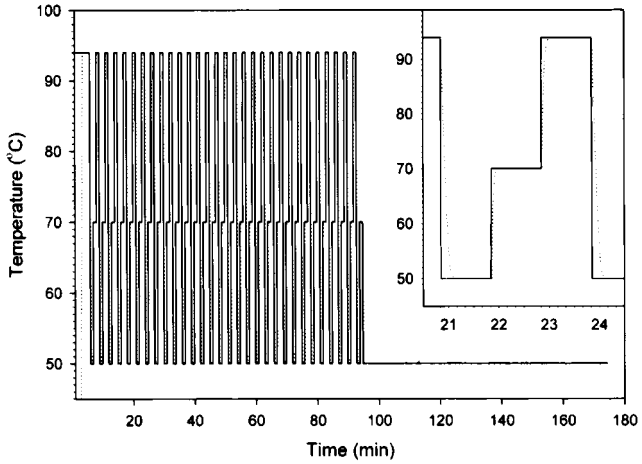

Figure 3. Graph of the temperature profile used for the combined PCR and hybridization experiment (—, set-point temperature; ---, measured temperature). The insert shows details of a single PCR cycle, demonstrating the superior accuracy and ramping speed of the temperature control.

in arrays with 200-μm spot distance and ~80-μm spot diameter and immobilized by disulfide formation. In our experiments, only the center part (1.6 × 0.8 mm^2) of the reactor floor was used for array printing (8 × 4 spots). However, array size and spot density can be increased easily (e.g., 2 × 3 mm^2 arrays featuring ~600 individual spots).

Following array printing, a glass wafer was bonded onto the silicon wafer containing inlet and outlet holes for filling the microreactor with reagents. Commonly used anodic bonding techniques require a temperature of >300 °C, which would damage the oligonucleotide microarray. UV-curable glue was used instead after ensuring that it did not inhibit PCR. Finally, the wafer was diced into single μ-DAAD's with a diamond saw (Figure 2B,C).

PCR Cycling. The temperature cycling of the PCR is illustrated in Figure 3. The measured temperature followed the set-point temperature with a short time delay because of the temperature capacity of the device. The insert of Figure 3 demonstrates the excellent temperature control, with a maximum deviation of ± 0.3 °C and a ramping speed of 2.9 °C/s for heating and 2.4 °C/s for cooling, respectively. After completion of the PCR cycles, the hybridization was performed by heating the reactor to the desired hybridization temperature (e.g., 50 °C).

Assay Results. Confocal fluorescent scans of the integrated microarrays are shown in Figure 4A−D. The Texas Red-labeled oligonucleotide no. 10 was immobilized as the reference sample serving as an indicator of the immobilization efficiency (column 7). The spot-to-spot variation in the amount of immobilized oligonucleotide was <12%. Detection of oligonucleotide no. 10 after PCR cycling demonstrated that the covalent attachment used for the microarray was heat-stable. An amount of 1.5 × 10^{-15} mol of genetic material from *Pinellia padatisecta* (PP) was added to reactor A, and genetic material from *Datura innoxia* (DI) was added to reactor B (see Figure 4). Following PCR and hybridization, fluorescent spots of high intensity were detected in columns 2 and 6 containing the probes corresponding to these TCMs. Low background fluorescence intensity was found in control experiments (not illustrated) where primers for PP and DI were present,

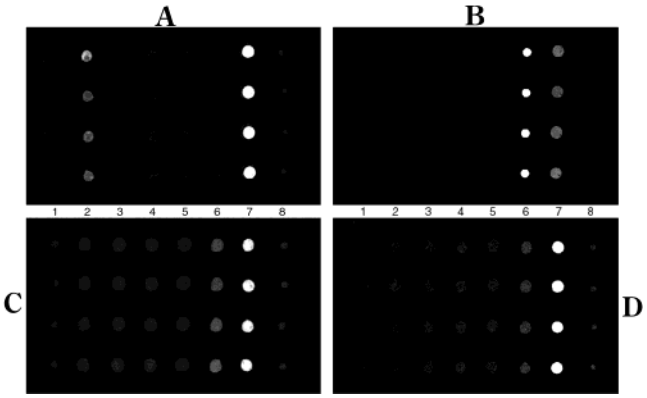

Figure 4. Confocal fluorescent scans of microarrays after the combined PCR and hybridization experiment. Arrays of eight columns with four spots each and a spot distance of 200 μm were printed. The arrays consist of three control columns and oligonucleotide probe columns for five different TCM plants (names and sequences are given in Table 1) in the following order (from left to right): (1) spotting buffer as negative control, (2) probe 23 for PP, (3) probe 28 for AM, (4) probe 33 for TG, (5) probe 42 for HF, (6) probe 88 for DI, (7) oligonucleotide 10 as immobilization control, and (8) spotting buffer only serving as a negative control. The hybridized PCR products are Texas-Red-labeled. (A) Genetic material (1.5×10^{-15} mol) of *P. padatisecta* (PP) was added. High spot intensity was found in column 2 printed with the corresponding probe of oligonucleotide 23. (B) Genetic material (1.5×10^{-15} mol) of *D. innoxia* (DI) was added. Because of the very high spot intensity found in the corresponding column 6 (printed with oligonucleotide 88), the scanner sensitivity was reduced in this experiment. (C, D) Lower amounts of genetic material (1.5×10^{-18} and 1.5×10^{-19} mol, respectively) of *D. innoxia* were added. Spot intensity was found to be proportional to the template concentration.

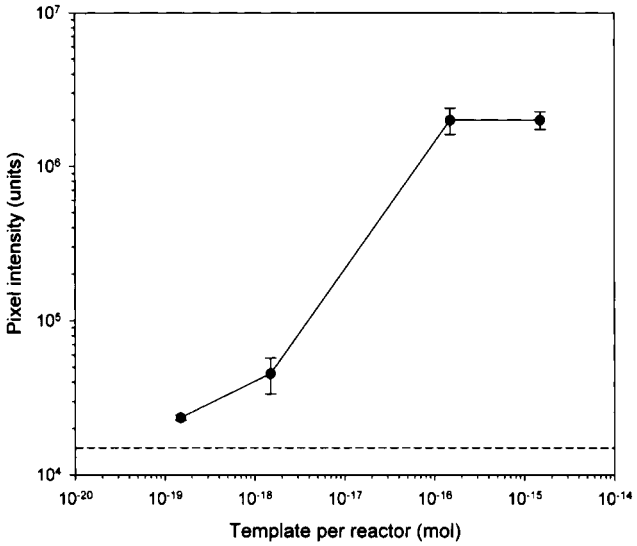

Figure 5. Spot intensities in dependence of template amount. The spot intensity for *D. innoxia* was proportional to the template concentration. As little as 1.5×10^{-19} mol template could be detected (signal-to-noise ratio of 2), corresponding to ~90 000 molecules/PCR reactor (3 μL sample volume). The dotted line represents the noise (unspecific hybridization of PCR products to spots of a nontarget species) of the experiment. Data points represent the mean ± standard deviation ($n = 4$).

but genetic material from TCM plants was omitted. The signal (specific hybridization)-to-noise (background signal at columns 1 and 8) ratio was determined to be >150. The signal (specific hybridization)-to-noise (unspecific hybridization at columns 3, 4, and 5) ratio was found to be >80, demonstrating the identification of 1.5×10^{-15} mol added TCM DNA. The signal-to-noise ratio was reduced to 4 after a decrease in the template concentration (DI) to 1.5×10^{-18} mol (Figure 4C). The smallest detectable amount of template was 1.5×10^{-19} mol, with a signal-to-noise ratio of 2 (Figure 4D). With an approximate size of 3×10^9 base pairs for the human genome (equivalent to $\sim 2 \times 10^{12}$g/mol), ~300 ng genomic DNA would contain 1.5×10^{-19} mol of a single copy gene. Thus, μ-DAAD-based genotyping using total genomic DNA is feasible.

Figure 5 demonstrates the dependence of the spot intensity (mean pixel value) on the template amount for *D. innoxia*. Amounts of 1.5×10^{-15} mol and 1.5×10^{-16} mol template resulted in similar signal intensity. This finding may be due to the complete incorporation of the fluorescence-labeled primer in the PCR product and the saturation of the probe with hybridized PCR product. The maximum amount of PCR product is similar to the amount of the fluorescent-labeled primer ($\sim 10^{-12}$ mol/reactor). We determined the amount of immobilized oligonucleotide to be 10^{-15} mol/species and reactor (the scanner was calibrated with a known amount of a fluorescent-labeled oligonucleotide, data not shown). Consequently, the maximal molar ratio between PCR product and immobilized probe can reach 1000:1 for high template concentrations. This can lead to a saturation of the probe oligonucleotide with no further signal increase.

We found a signal increase with increasing number of PCR cycles for low template amounts. The forward primer amount (1.2×10^{-14} mol/reactor) was ~10 times higher than the amount of immobilized oligonucleotide. Forward primers and probes compete with each other in their hybridization to PCR products. A molar excess of PCR product to the sum of immobilized oligonucleotide and forward primer ($\sim 1.3 \times 10^{-14}$ mol) is necessary to generate a sufficient signal. To produce $\sim 1.3 \times 10^{-14}$ mol of PCR product from as little as 1.5×10^{-19} mol template, an amplification factor of $\sim 10^5$ is necessary. Theoretically, a minimum of 17 PCR cycles ($2^{17} \approx 10^5$) plus 3 initial cycles is needed. In practice, we found that 36 PCR cycles was sufficient to generate a detectable signal. Hybridization of PCR product to immobilized oligonucleotide probes takes place at a solid phase; in contrast, the hybridization to the forward primers takes place in a homogeneous phase. Diffusion and kinetic effects may lead to a reduced efficiency of the probe hybridization. We found the following molar ratios of the reaction compounds were optimal under the conditions of our experiment: 1× immobilized probe (10^{-15} mol)/10× forward primer (10^{-14} mol)/200−1000× fluorescent-labeled primer (0.2×10^{-12} to 10^{-12} mol)/10^{-4} to 1× template (10^{-19} to 10^{-15} mol), resulting in maximal 200−1000× PCR product.

The possible elongation of the oligonucleotide probes during PCR[11] has not been confirmed yet and is the subject of further studies. We anticipate that assays that make use of immobilized primers in a "primer/probe array" setup have some potential advantages. When compared with common PCR in which all

(11) Erdogan, F.; Kirchner, R.; Mann, W.; Ropers, H. H.; Nuber, U. A. *Nucleic Acids Res.* **2001**, *29*, E36.

primers, templates, and amplified product are in solution, a primer bound to the surface can potentially create a "microreaction spot". Less interference is expected between parallel reactions in multiple microreaction spots during multiplex PCR. Quantitative readout of the integrated microarray might be further improved by the use of a two-color system in which the hybridization data is normalized for each spot in relation to the amount of immobilized probe, thus reducing the influence of spot-to-spot variation due to unequal immobilization.

The integration density of microreactors in the μ-DAAD can be easily increased.[12] Currently, the limiting factors are sample application and selective filling of individual reactors. No restrictions of the available silicon technology limit the realization of much smaller feature sizes. With advanced filling techniques, reactor volumes can be reduced to 0.1 to 1 μL, allowing an increase in reactor integration density. Arrays of 5×5 reactors/cm^2, each containing a DNA microarray with, for example, 10×10 spots could perform 25 analyses in parallel, each targeting 100 sequences.

CONCLUSION

We report on the integration of PCR with a DNA microarray into a single Si-based device and demonstrate its application for the genotyping of Chinese medicinal plants. A fully wafer-based production sequence was developed, including a "biocompatible" bonding process. Microreactors, heaters, and temperature sensors were fabricated in a CMOS compatible process, followed by microarray printing. Because of the small heat capacity, fast and accurate PCR thermocycling is achieved, and only little energy is needed (max, 2.5 W). Washing volumes are small (3−10 times the reactor volume), making the device suitable for mobile instrumentation. μ-DAAD-based genotyping of 10^{-19} mol of starting material was demonstrated. Our approach of combining PCR amplification of genetic material with consecutive analysis is a further step toward the creation of a "lab-on-a-chip".

ACKNOWLEDGMENT

This work was supported by grants from the Innovation & Technology Commission of the Hong Kong SAR (AF/150/99) and the Hong Kong Jockey Club. The authors thank Dr. Karl Tsim for providing TCM DNA and sequences, Kin Lok Cheung and Fei Cao for help with control experiments and microarray printing, and Mr. Kwok Kei Lau for his support in machining of the glass wafers.

Received for review January 28, 2002. Accepted March 26, 2002.

AC020053U

(12) Nagai, H.; Murakami, Y.; Morita, Y.; Yokoyama, K.; Tamiya, E. *Anal. Chem.* **2001**, *73*, 1043−1047.